

See discussions, stats, and author profiles for this publication at: <https://www.researchgate.net/publication/230703886>

Molybdenum Oxide Thin Films Obtained by the Hot-Filament Metal Oxide Deposition Technique

ARTICLE in CHEMISTRY OF MATERIALS · FEBRUARY 2004

Impact Factor: 8.35 · DOI: 10.1021/cm034551a

CITATIONS

38

READS

16

7 AUTHORS, INCLUDING:



Francisco Paulo Rouxinol

Syracuse University

36 PUBLICATIONS 195 CITATIONS

SEE PROFILE



Steven F. Durrant

São Paulo State University

110 PUBLICATIONS 1,332 CITATIONS

SEE PROFILE



J. Scarminio

Universidade Estadual de Londrina

37 PUBLICATIONS 367 CITATIONS

SEE PROFILE



Alexandre Urbano

Universidade Estadual de Londrina

29 PUBLICATIONS 142 CITATIONS

SEE PROFILE

Molybdenum Oxide Thin Films Obtained by the Hot-Filament Metal Oxide Deposition Technique

Mario A. Bica de Moraes,* B. Cláudio Trasferetti, Francisco P. Rouxinol, and Richard Landers

Departamento de Física Aplicada, Instituto de Física Gleb Wataghin, Universidade Estadual de Campinas, 13083-970, Campinas, SP, Brazil

Steven F. Durrant

Universidade do Vale do Paraíba, Laboratório de Deposição a Vapor Químico, Instituto de Pesquisa e Desenvolvimento, Av. Shishima Hifumi, 2911, Urbanova, 12244-000, São José dos Campos, SP, Brazil

Jair Scarmínio and Alexandre Urbano

Departamento de Física, Universidade Estadual de Londrina, 86051-990, Londrina, PR, Brazil

Received June 27, 2003. Revised Manuscript Received September 29, 2003

Molybdenum oxide thin films find diverse applications as catalysts, gas sensors, and electrochromic devices. Such films are produced mainly by reactive sputtering and thermal evaporation but other techniques such as chemical vapor deposition and electrochemical deposition have been used. In the present work, the feasibility of an alternative method for the production of molybdenum oxide films using a molybdenum filament heated in a rarefied oxygen atmosphere is demonstrated. The filament heating current, I_F , and the oxygen flow rate, F_{O_2} , are the key deposition parameters and their effect on the deposition rate, R , was investigated. For $I_F = 12.5$ A, an increase in the R -value from 7.5 to 31 nm/min was observed as F_{O_2} was increased from 6.0 to 21 sccm. To characterize the chemical bonds, infrared spectroscopy, using both unpolarized and p-polarized infrared beams, and X-ray photoelectron spectroscopy (XPS) were employed. Line shape analysis of the Mo(3d) XPS peak revealed that the Mo atoms were in mixed valence states, Mo^{6+} and Mo^{5+} , with a high predominance of the former over the latter, thus indicating an oxygen-deficient MoO_3 film. From Rutherford backscattering spectroscopic analysis of the films, an average O/Mo atomic ratio of 2.9 was calculated, consistent with the XPS results. A combination of the XPS and RBS results and the data of other investigators on the oxidation of molybdenum suggests that the film is formed from MoO_2 and MoO_3 species desorbed from the Mo filament. The optical gap, E_g , was determined from transmission UV–visible spectra of the films. An average E_g value of 3.03 eV was found. The electrochromic properties of the films were investigated for Li^+ intercalation using an electrochemical cell. A coloration efficiency of 19.5 cm^2/C at a wavelength of 700 nm was observed.

Introduction

The singular structural, electrical, and optical properties of thin molybdenum oxide films have led to several interesting applications. Molybdenum oxide exhibits electrochromism; that is, a change in color may be produced by the intercalation of ions such as Li^+ and H^+ .¹ As the intercalation process is usually reversible and controllable, the application of these films to optical devices such as panel displays² and “smart windows”³ is very promising. Owing specifically to the high revers-

ibility of the intercalation of Li^+ , another remarkable potential application of Mo oxide films is in high-energy density microbatteries.⁴

Since most Mo oxide films are semiconductors, and the surface adsorption of some molecular species produces changes in their electrical conductivity, several studies of molybdenum oxide films as gas-sensing devices have been performed. For detection of CO^5 and NO^6 sensitivities as high as 10 ppm in air have been reported. Furthermore, molybdenum oxide surfaces exhibit a strong catalytic action and can be used to

* Corresponding author: bmoraes@ifi.unicamp.br

(1) Granqvist, C. G. *Handbook of Inorganic Electrochromic Materials*; Elsevier: Amsterdam, 1995.

(2) Miyata, N.; Susuki, T.; Ohyama, R. *Thin Solid Films* **1996**, 281/282, 218.

(3) Lampert, C. M. *Sol. Energy Mater.* **1984**, 11, 1.

(4) Julien, C.; Yebka, P.; Guesdon, J. P. *Ionics* **1995**, 1, 316.

(5) Ferroni, M.; Guidi, V.; Martinelli, G.; Nelli, P.; Sacerdoti, M.; Sberveglieri, G. *Thin Solid Films* **1997**, 307, 148.

(6) Di Giulio, M.; Manno, D.; Micocci, G.; Serra, A.; Tepore, A. *Phys. Status Solidi A* **1998**, 168, 249.

promote reactions such as nitrite oxidation⁷ and the partial oxidation of organic molecules.⁸

To date, molybdenum oxide films have been obtained by various techniques, such as magnetron⁹ and rf sputtering,¹⁰ flash¹¹ and thermal evaporation,¹² CVD,¹³ electrodeposition,¹⁴ and spin coating.¹⁵ As expected, the film structure and properties differ from one deposition method to another. Even with use of the same technique or indeed the same deposition system, however, widely different structures and stoichiometries can be obtained by changing the deposition parameters.

Recently, a new deposition method, which we call hot filament metal oxide deposition (HFMOD), has been investigated in our laboratory. In this technique, a metal filament is heated in a low-pressure oxygen atmosphere and the film is formed, on a substrate positioned near the filament, from volatile metal oxide species generated on the filament surface from reactions with oxygen. Tungsten oxide films of high electrochromic efficiency, obtained by HFMOD, were reported in a previous publication.¹⁶ In this paper we describe an investigation of molybdenum oxide films deposited by this technique. The oxygen flow rate to the chamber, F_{O_2} , and the filament heating current, I_F , were the fundamental parameters used to control the deposition rate. With use of a number of characterization techniques, the crystalline state, morphology, molecular structure, and optical gap of the films were studied. The electrochromic effect of Li^+ intercalation was also investigated.

Experimental Section

Film depositions were carried out in a stainless steel vacuum chamber fitted with a Mo filament and pumped by a $150\text{ m}^3\text{ h}^{-1}$ roots pump. The filament, the substrate, and substrate holder are shown schematically in Figure 1. The filament was resistively heated by an ac current from an ac power supply while an ammeter was used to measure the current. A quartz viewport in the chamber allowed the filament temperature to be measured using a precision optical pyrometer. Temperature readings were corrected assuming a molybdenum emissivity of 0.37. The temperature of the substrate holder was measured using a chromel alumel thermocouple. Water circulation in the copper plate sustaining the substrate holder (Figure 1) prevented excessive heating of the substrate during film deposition. The purity of the molybdenum wire filament, as determined by electron probe microanalysis, was greater than 99.9%. To admit oxygen to the chamber, an electronic precision mass flowmeter was used while the pressure was monitored using a capacitance manometer. The purity of the oxygen was greater than 99.999%.

To measure the film thickness, a small circular ink mark was initially made on the substrate with a felt-tip pen.

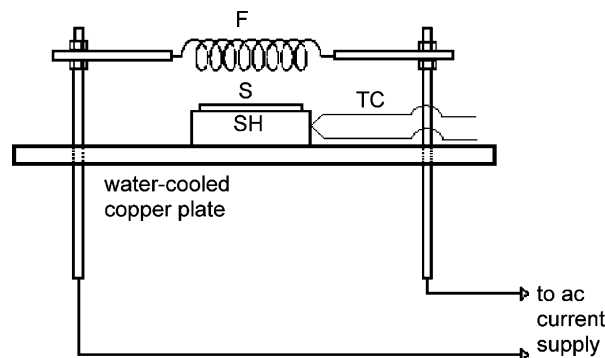


Figure 1. Schematic representation of the experimental arrangement inside the chamber. F, filament of 0.6-mm-diameter molybdenum wire, shaped into a seven-turn coil of 8-mm diameter and 35-mm length; S, substrate; SH, copper substrate holder of $50 \times 30 \times 7\text{ mm}^3$; TC, thermocouple; filament-to-substrate separation, 30 mm.

Following deposition, the film above the mark was readily removed with acetone, and the depth of the hole, or the film thickness, was then measured using a high-resolution profilometer. The deposition rate was determined by the ratio of the film thickness to the deposition time.

X-ray diffraction (XRD) and scanning electron microscopy (SEM) were used to investigate, respectively, the crystalline structure and the morphology of films deposited onto single-crystal Si substrates. The X-ray diffractometer operated in the θ - 2θ mode with the monochromatized $\text{Cu K}\alpha$ line of 0.154098 nm.

Studies of the chemical bonds in the films were undertaken using Fourier transform infrared spectroscopy (FTIR) in the reflection-absorption mode and X-ray photoelectron spectroscopy (XPS). The FTIR spectra covered the $400\text{--}4000\text{ cm}^{-1}$ range at a resolution of 4 cm^{-1} and were taken from films deposited onto Al-coated glass substrates. Unpolarized and p-polarized IR beams were used. A variable-angle attachment was employed, at the incidence angles of 10, 30, 50, and 70° off-normal for p-polarized radiation. All spectra were referenced to a bare Al-coated glass substrate.

To obtain the XPS spectra, a hemispherical analyzer was employed, using the unmonochromatized Al $\text{K}\alpha$ X-ray line (1487 eV) for photoelectron excitation. To investigate the various possible oxide stoichiometries in the films, Mo(3d) core level spectra were obtained and spectral analysis was carried out using Gaussian curves to fit the experimental data.

Composition analyses of the films were carried out using Rutherford backscattering spectroscopy (RBS) at the Laboratory for Analysis of Materials by Ion Beams—LAMFI of the Institute of Physics, University of São Paulo. A beam of singly ionized 2.4 MeV helium atoms aligned normal to the film surface was used with detection at 7° off-normal. Single-crystal (100) Si wafers were used as substrates. The RUMP computational program¹⁷ was applied to the RBS data to obtain the O/Mo atomic ratios.

From the transmission spectra taken with an ultraviolet-visible spectrophotometer, the absorption coefficient was determined using a procedure described in a previous publication.¹⁸ For these analyses, films were deposited onto quartz substrates.

An airtight electrochemical cell controlled by a potentiostat and coupled with an optical spectrometer and tungsten light source was used to investigate the electrochromic properties of films upon Li^+ intercalation. Silver and platinum wires were used as the reference electrode and the counter electrode, respectively, while the oxide film was the working electrode. The electrolyte (LiCl_4 in 1.0 M propylene carbonate) and the cell were handled in a closed dry argon atmosphere. Glass

(7) Rocha, J. R. C.; Kosminsky, L.; Paixão, T. R. L. C.; Bertotti, M. *Electroanalysis* **2001**, *13*, 155.

(8) Firment, L. E.; Ferretti, A. *Surf. Sci.* **1983**, *129*, 155.

(9) Kharrazi, M.; Azens, A.; Kullman, L.; Granqvist, C. G. *Thin Solid Films* **1997**, *295*, 117.

(10) Scarminio, J.; Lourenço, A.; Gorenstein, A. *Thin Solid Films* **1997**, *302*, 66.

(11) Julien, C.; Hussain, O. M.; El-Fahr, L.; Balkanski, M. *Solid State Ionics* **1992**, *53–6*, 400.

(12) Quevedo-Lopez, M. A.; Mendoza-Gonzalez, O.; Reidy, R. F.; Ramirez-Bon, R.; Orozco-Teran, R. A. *J. Phys. Chem. Solids* **2000**, *61*, 727.

(13) Abdellaoui, A.; Lévêque, G.; Donnadieu, A.; Bath, A.; Bouchikhi, B. *Thin Solid Films* **1997**, *304*, 39.

(14) Guerfi, A.; Dao, L. H. *J. Electrochem. Soc.* **1989**, *136*, 2435.

(15) Hinokuma, K.; Kishimoto, A.; Kudo, T. *J. Electrochem. Soc.* **1994**, *141*, 876.

(16) Scarminio, J.; Bica de Moraes, M. A.; Dias, R. C.; Rouxinol, F. P.; Durrant, S. F. *Electrochem. Solid State Lett.* **2003**, *6*, H9.

(17) Doolittle, J. R. *Nucl. Instrum. Methods B* **1985**, *9*, 334.

(18) Durrant, S. F.; Castro, S. G.; Cisneros, J. I.; da Cruz, N. C.; Bica de Moraes, M. A. *J. Vac. Sci. Technol. A* **1996**, *14*, 118.

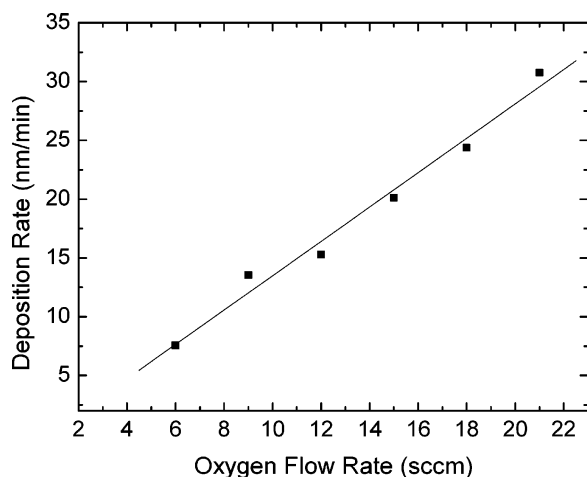


Figure 2. Deposition rate as a function of the oxygen flow rate. Filament current: 12.5 A. Filament temperature: 1800 K.

slides with a transparent conductive indium–tin oxide layer coating were used as substrates.

Results and Discussion

Deposition Rate. Figure 2 shows the film deposition rate, R , as a function of the oxygen flow rate, F_{O_2} , for a constant filament current, I_F , of 12.5 A. Clearly, R increases monotonically with increasing F_{O_2} , as a consequence of the increasing rate of formation of molybdenum oxide with the increase in the oxygen pressure in the chamber. A fairly large R -value is obtained (31 nm min^{-1}) for the O_2 flow rate of 21 sccm but even at 6.0 sccm the deposition rate is appreciable. In all depositions undertaken to obtain the data of Figure 2, the measured molybdenum filament temperature was 1800 K and the deposition time varied from 14 to 18 min. Despite the close proximity of the filament to the substrate, the temperature of the copper substrate holder did not exceed 318 K. As glass substrates were used for the R -measurements, their maximum surface temperatures were probably greater than this, due to their low thermal conductivity. As will be discussed below, however, the substrate temperature did not exceed 550 K in the deposition of any of the films investigated in this work. Thus, this deposition technique is suitable to obtain molybdenum oxide films on substrates that may not withstand high temperatures, such as polymers and indium tin oxide-covered glass slides.

In a series of depositions in which the O_2 flow rate was kept constant at 15 sccm, the deposition rate was measured as a function of the filament current. For each deposition, the filament temperature was also recorded. The results are depicted in Figure 3, revealing an increase in R with increasing I_F , or equivalently, with increasing filament temperature. As before, this behavior is explained by an increase in the reaction rate between oxygen and molybdenum, this time due to the increasing temperature.

Since Mo atoms are lost from the filament during the deposition process, it is of interest to define the relative mass loss rate of the filament, given by the expression $\beta = (A/M_F)(\Delta m_F/\Delta t)$, where A is the filament surface area, M_F is the filament mass, and $\Delta m_F/\Delta t$ is the mass

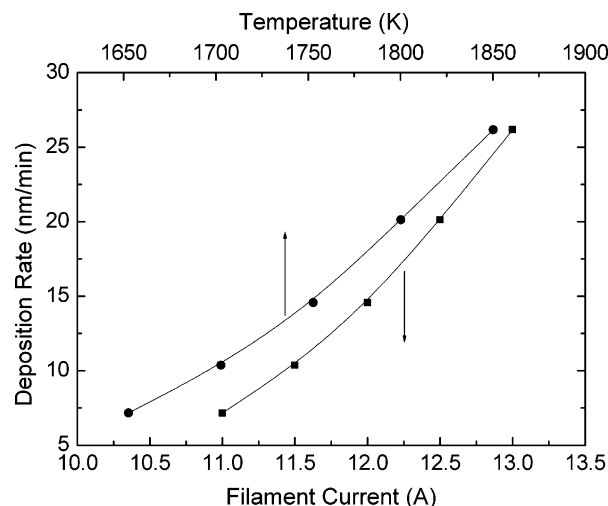


Figure 3. Deposition rate as a function of the filament current and filament temperature. Oxygen flow rate: 15 sccm. The arrows indicate the filament current and the temperature scale for each curve.

loss per unit area per unit time. For a given Mo filament, the $(\Delta m_F/\Delta t)$ ratio can be determined experimentally at a given temperature and oxygen flow rate and then applied to the expression for β which now holds for any Mo filament at the same temperature and flow rate, regardless of diameter and shape. The β -parameter is useful in evaluating filament lifetime since there is an obvious practical interest in using a filament capable of surviving several depositions. It is also useful as an indication of the change in the deposition rate during the deposition process since, as the filament becomes thinner, due to mass loss, its electrical resistance is increased and its surface area is decreased. For a constant current applied to the filament, both changes affect the deposition rate: the filament temperature increases due to the increased electrical resistance while the total number of Mo surface atoms decreases due to the decreased surface area.

For depositions under the conditions used here, however, the β -values were usually low, implying, for a constant filament current, a nearly constant deposition rate over fairly long times. From a measurement of the mass difference of a filament operating for 2 h at $I_F = 12.5 \text{ A}$ and $F_{O_2} = 18 \text{ sccm}$, a β -value of 0.03 min^{-1} was found. This implies in percent mass and filament diameter decreases of only 3% and 1.5%, respectively, for each hour of operation.

Gas-Phase Species Desorbed from the Filament.

Reactions between adsorbed oxygen originating from the gas phase and the Mo atoms of the filament surface may result in adsorbed Mo oxide species. Clearly, the rate of formation of these species, their stoichiometry, and their rates of desorption depend on the filament temperature and on the oxygen pressure. The complete formation–desorption scheme is complicated since (i) different oxide species may be formed prior to desorption and (ii) oxide species with different stoichiometries may be present in the vapor flux, some resulting from dissociation of the species originally formed.

The Mo oxide species desorbing from a Mo surface heated in an oxygen atmosphere were analyzed by Berkowitz-Mattuck et al.¹⁹ using a mass spectrometer. At temperatures of about 1300 K and a pressure of

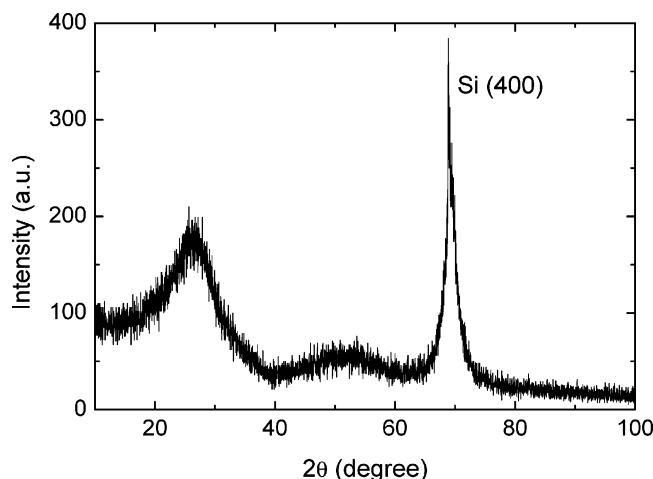


Figure 4. X-ray diffraction spectrum of a molybdenum oxide film deposited onto a single Si crystal substrate. The sharp peak near 70° is due to the Si substrate. Deposition parameters: $I_F = 12.5$ A, $F_{O_2} = 21$ sccm. Film thickness: 620 nm.

nearly 1 Pa, the gas-phase species $(\text{MoO}_3)_2$, MoO_3 , and MoO_2 were observed. For temperatures and pressures in the ranges 1500–1900 K and 0.08–1.15 Pa, respectively, $(\text{MoO}_3)_2$ disappeared from the gas phase and the only detected desorbed oxide species were MoO_2 and MoO_3 , with a predominance of the latter.

In the present work, the data for Figures 2 and 3 were obtained at oxygen pressures in the 0.75–2.0 Pa interval and at temperatures between 1650 and 1860 K. Since this temperature interval is in the temperature range of the experiments reported in ref 19, and the maximum pressure we used (2.0 Pa) does not widely differ from that given in the latter (1.15 Pa), it seems reasonable to assume that the only oxide species desorbing from the filament at significant rates were MoO_3 and MoO_2 , with the former predominating. Since the film grows mainly from the oxide species desorbed from the filament, an overall MoO_x stoichiometry, with x larger than 2 but smaller than 3 is expected. As film growth takes place in an oxygen atmosphere, however, chemical incorporation of oxygen atoms into the film is possible, forming new Mo–O bonds, which may further increase x to values closer to 3.

Structure and Morphology. Figure 4 shows a typical XRD spectrum of a molybdenum oxide film deposited onto a single-crystal Si substrate. The thickness of the film was 620 nm, and for crystalline Mo oxide films, this thickness would be sufficient to exhibit diffraction peaks in the 2θ region between 10° and 100° . The absence of the oxide peaks in the spectrum and the broad diffuse background between 10° and 40° reveals that the film is amorphous.

Structural investigations of molybdenum oxide films obtained by thermal evaporation,¹² rf sputtering,²⁰ and spin coating²¹ reveal that thermally treated amorphous films are converted to crystalline at temperatures between 520 and 550 K. Since our films are amorphous, these results indicate that, despite the close proximity

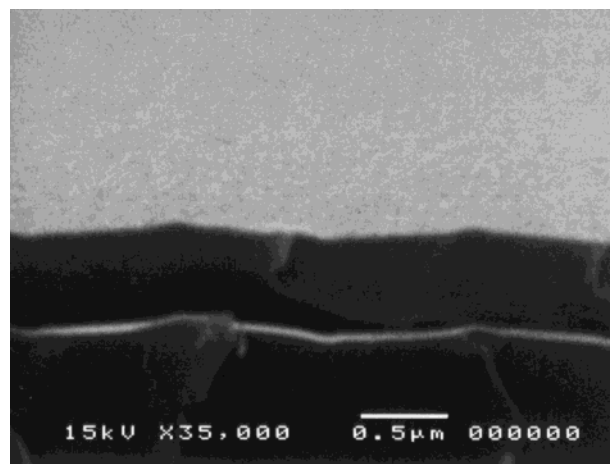


Figure 5. SEM micrographs of a fractured film. Deposition parameters: $I_F = 12.5$ A, $F_{O_2} = 15$ sccm.

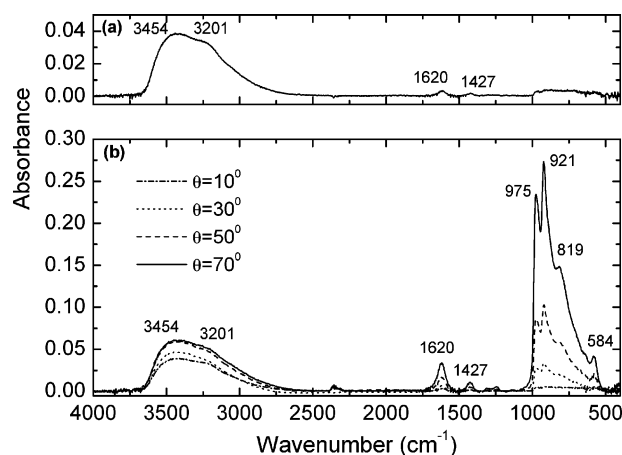


Figure 6. FTIR reflection-absorption spectra: (a) acquired at an incidence angle of 10° using unpolarized light; (b) acquired at various incidence angles using p-polarized light. Deposition parameters: $I_F = 12.5$ A, $F_{O_2} = 15$ sccm. Film thickness: 240 nm.

of the filament, the substrate temperature remains below 550 K.

The SEM pictures shown in Figure 5 represent the typical morphology of the films. The film surface is rather smooth and uniform while the fracture cross section reveals a structureless and compact material.

FTIR Analysis. Figure 6a exhibits the FTIR absorbance spectrum of a film taken in the conventional (unpolarized) mode at an incidence angle of 10° and Figure 6b shows spectra of the same sample acquired using p-polarized light at different incidence angles. Several absorption bands between 500 and 4000 cm^{-1} can be seen in the spectra. While the bands in the $500\text{--}1100\text{ cm}^{-1}$ region are rather weak in the conventional spectrum, those of the spectra obtained with p-polarized light are intense and strongly increase as the incidence angle is increased. According to several investigators,^{22–28} stretching bands related to Mo–O bonds occur in this region. Since both longitudinal (LO) and transversal (TO) modes can be detected when oblique incidence and

(19) Berkowitz-Mattuck, J. B.; Büchler, A.; Engelke, J. L.; Goldstein, S. N. *J. Chem. Phys.* **1963**, *39*, 2722.

(20) Garcia, P. F.; McCarron, III, M. *Thin Solid Films* **1987**, *155*, 53.

(21) Gaigneaux, E. M.; Fukui, K.; Iwasawa, Y. *Thin Solid Films* **2000**, *374*, 49.

(22) Beattie, I. R.; Gilson, T. R. *J. Chem. Soc. A* **1969**, 2322.

(23) Py, M. A.; Schmid, P. E.; Vallin, J. T. *Il Nuovo Cimento* **1977**, *38 B*, 271.

(24) Nazri, G. A.; Julien, C. *Solid State Ion.* **1992**, *53–56*, 376.

p-polarized light are used,^{29–31} band assignments are not straightforward. Comparing our results with those of Py and co-workers,²³ however, the assignment of the bands at ~ 819 and ~ 975 cm^{-1} to an LO–TO pair related to the symmetrical stretching of MoO_2 groups seems acceptable.

Apart from the band envelope in the $500\text{--}1100\text{-cm}^{-1}$ range, bands at ~ 1427 , ~ 1620 , and ~ 3454 cm^{-1} are present in the spectra and they originate from water incorporation into the film. The band at ~ 1620 cm^{-1} can be assigned to the deformation mode of H_2O . Its position, above the gas-phase value³² of 1595 cm^{-1} and below that of liquid water³³ (1640 cm^{-1}), indicates the presence of H_2O molecules in a network of hydrogen bridges. The band at ~ 1427 cm^{-1} can be attributed to the OHO bending vibration of molybdenum hydrates.²⁶ Minor bands observed in the $1000\text{--}1300\text{-cm}^{-1}$ range have been attributed to combination modes of optical phonons of intermediate energy.²⁶

The hydrous character observed in our films was also noted by other investigators³⁴ in molybdenum oxide films obtained by magnetron sputtering. In their FTIR study using p-polarization, they pointed out the existence of a broad infrared band at around 3500 cm^{-1} , probably associated with OH bonds.

Since the bands related to Mo–O bonds are hardly discernible in the conventional spectrum (Figure 6a), the above-described FTIR results clearly illustrate the usefulness of p-polarized light to investigate, and even to identify, molybdenum oxide thin films.

XPS Analysis. Owing to the higher electronegativity of oxygen compared to that of molybdenum, the electron binding energies of the molybdenum core levels increase as the metal bonds to oxygen. Molybdenum atoms may combine with oxygen in a number of valence states, $\text{Mo}^{\delta+}$, with δ in the range from 1 to 6 and the binding energies of the core electrons increase as δ is increased.

In Figure 7, the XPS spectrum of the Mo3d levels is represented for a molybdenum oxide film deposited onto a Si substrate using a filament current and an oxygen flow rate of 12.5 A and 18 sccm, respectively. The experimental data, represented by the squares, clearly shows the characteristic Mo(3d) doublet, composed of the $3d_{5/2}$ and $3d_{3/2}$ levels produced by spin–orbit coupling. Good fitting of the data points is made using two pairs of Gaussian functions, corresponding to two possible 3d doublets of molybdenum in different oxidation states. The major contribution to the spectrum is given by the pair whose Gaussians are peaked at 232.7 and 235.8 eV, identified as the energies of the 3d doublet of

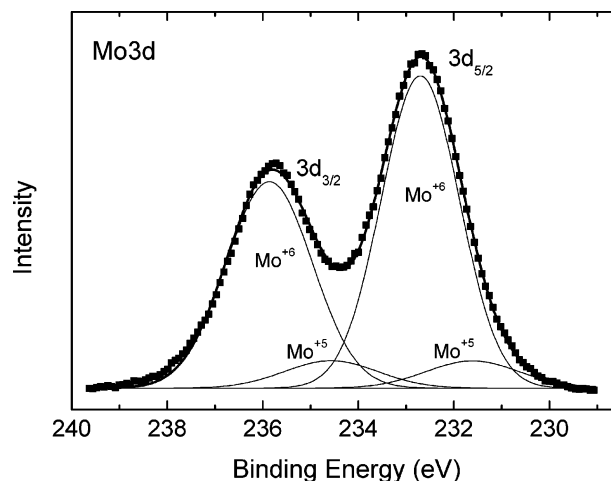


Figure 7. XPS spectrum of the Mo(3d) core levels for a film deposited with $I_f = 12.5$ sccm and $F_{O_2} = 18$ sccm. The thicker line is the fitting of the experimental data (squares) by the Gaussian peaks (thin lines).

Mo^{6+} . The other pair, with peak energies of 231.6 and 234.6 eV, is assigned to the 3d doublet of Mo^{5+} . For both Mo^{6+} and Mo^{5+} , these binding energies are in close agreement with literature values.^{35–37} From the ratio of the areas of the two Gaussian pairs, the value of 0.11 is obtained for the ratio of the number of Mo^{5+} atoms to the total Mo atoms in the sample. Thus, the film is in the MoO_3 stoichiometry, with a small oxygen deficiency.

These results are consistent with the idea discussed previously that MoO_2 and MoO_3 are the only important species desorbing from the Mo filament. Although oxygen from the chamber may be chemically incorporated into the film and further oxidize Mo^{5+} atoms, the fact that the film stoichiometry is close to that of MoO_3 is in agreement with our expectation that the desorption rate of the MoO_3 species is higher than that of MoO_2 .

The Mo(3d) spectrum of a film obtained with the same filament current as before (12.5 A) but with a lower oxygen flow rate (6.0 sccm) can also be fitted with two pairs of Gaussian peaks at nearly the same energies as those of Figure 7. The ratio of the areas of the two pairs of Gaussian peaks is also close to 0.11 . Although we have not taken XPS data for F_{O_2} values other than 6.0 and 18 sccm, these results suggest that, in the range from 6.0 to 18 sccm, the film composition does not depend on the oxygen flow rate. It should be remembered, however, that as shown in Figure 2, the deposition rate varies strongly with F_{O_2} .

RBS Analysis. To investigate film stoichiometry using RBS, several samples were prepared employing a filament current of 12.5 A and oxygen flow rates from 6.0 to 21 sccm. A typical RBS spectrum of these samples is exhibited in Figure 8 and shows the characteristic edges due to molybdenum, oxygen, and silicon from the substrate. Table 1 displays the O/Mo atomic ratio of each sample, calculated using the RUMP program. The average of the O/Mo values is 2.9 , consistent with an

(25) Julien, C.; Khelfa, A.; Hussain, O. M.; Nazri, G. A. *J. Cryst. Growth* **1995**, *156*, 235.

(26) Mestl, G.; Srinivasan, T. K. K.; Knözinger, H. *Langmuir* **1995**, *11*, 3795.

(27) Nart, F. C.; Kelling, S.; Friend, C. M. *J. Phys. Chem. B* **2000**, *104*, 3212.

(28) Ivanova, T.; Szekeres, A.; Gartner, M.; Gogova, D.; Gesheva, K. A. *Electrochim. Acta* **2001**, *46*, 2215.

(29) Berreman, D. W. *Phys. Rev.* **1963**, *132*, 2193.

(30) Trasferetti, B. C.; Davanzo, C. U.; da Cruz, N. C.; Bica de Moraes, M. A. *Appl. Spectrosc.* **2000**, *54*, 687.

(31) Trasferetti, B. C.; Davanzo, C. U.; Zoppi, R. A.; da Cruz, N. C.; Bica de Moraes, M. A. *Phys. Rev. B* **2001**, *64*, 125404.

(32) Morrow, B. A. In *Studies in Surface Science*; Fierro, J. L., Ed.; Elsevier: Amsterdam, 1990; Vol. 57, p 161.

(33) Bertie J. E.; Lan, Z. *Appl. Spectrosc.* **1996**, *50*, 1047.

(34) Kharrazi, M.; Kullman, L.; Granqvist, C. G. *Sol. Energy Mater. Sol. Cells* **1998**, *53*, 349.

(35) Fleisch, T. H.; Mains, G. J. *J. Chem. Phys.* **1982**, *76*, 780.

(36) Colton, R. J.; Guzman, A. M.; Rabalais, J. W. *J. Appl. Phys.* **1978**, *49*, 409.

(37) Wagner, C. D.; Riggs, W. M.; Davis, L. E.; Moulder, J. F.; Muilenberg, G. E. In *Handbook of X-Ray Photoelectron Spectroscopy*; Perkin-Elmer: Eden Prairie, MN, 1979.

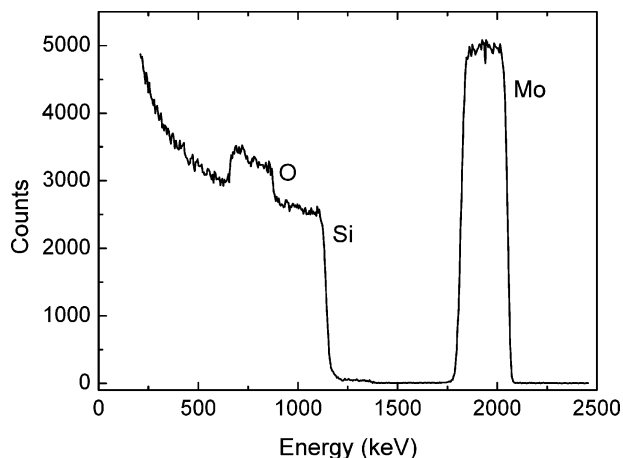


Figure 8. RBS spectrum for a film deposited with $I_F = 12.5$ A and $F_{O_2} = 15$ sccm.

Table 1. O/Mo Atomic Ratio Determined by RBS and Optical Gap of Samples Prepared with the Filament Current of 12.5 A and Various Oxygen Flow Rates

F_{O_2} (sccm)	O/Mo	E_g (eV)	F_{O_2} (sccm)	O/Mo	E_g (eV)
6.0	2.86	2.96	15	2.87	3.05
9.0	2.76	2.99	18	3.11	3.02
12	2.97	3.05	21	3.09	3.08

oxygen-deficient MoO_3 film, as indicated by the XPS results. However, water can be incorporated into the films, as shown by the previous FTIR analysis. Since the RBS technique is not sensitive to the chemical bonds of the atoms, the contribution of the O atoms in the water molecules adds to that of the O atoms bound to Mo, in the overall O/Mo atomic ratios of Table 1. This implies that the O/Mo atomic ratios due exclusively to the Mo oxide phase should exhibit lower values than those displayed in the table. Furthermore, there is no well-defined trend in the O/Mo atomic ratio as the oxygen flow rate varies. Thus, as already suggested by the XPS data, in the F_{O_2} range investigated, the film stoichiometry does not depend on F_{O_2} .

Optical Gap. To measure the optical gap, a series of films were deposited with the filament current of 12.5 A and oxygen flow rates ranging from 6.0 to 21 sccm, as indicated in Table 1. The UV-vis transmission spectra of the films obtained with the oxygen flow rates of 12 and 21 sccm are exhibited in Figure 9. Both spectra show maxima and minima due to light interference. Typical of the spectra of all films of the series is the steep edge between 250 and 400 nm, due to strong ultraviolet absorption and the minimum at about 900 nm, due to color centers.³⁸

The absorption coefficient, α , was calculated as a function of the photon energy, E , from the transmission UV-vis spectra. From the knowledge of $\alpha(E)$, the optical gap, E_g , was determined using Tauc's method,³⁹ which consists of plotting $(\alpha E)^{1/2}$ vs E and obtaining E_g by extrapolation of the linear portion of the graph to $(\alpha E)^{1/2} = 0$. The Tauc plot for the film deposited with $I_F = 12.5$ A and $F_{O_2} = 12$ sccm is shown in Figure 10 and extrapolation to $(\alpha E)^{1/2} = 0$ yields an E_g -value of 3.05 eV. The

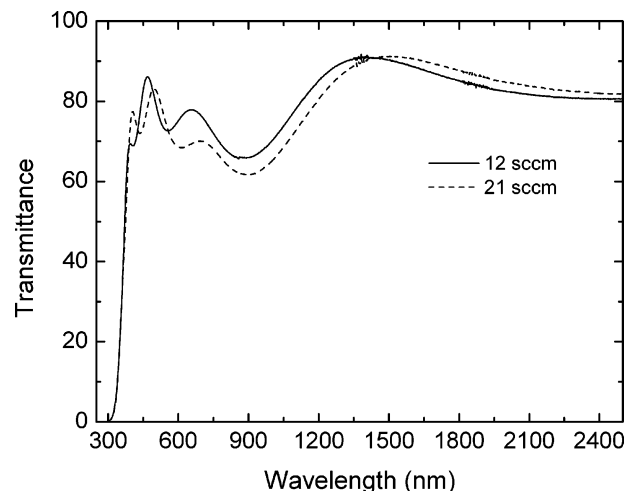


Figure 9. Optical transmittance as a function of photon wavelength for two films deposited with $I_F = 12.5$ A at different oxygen flows.

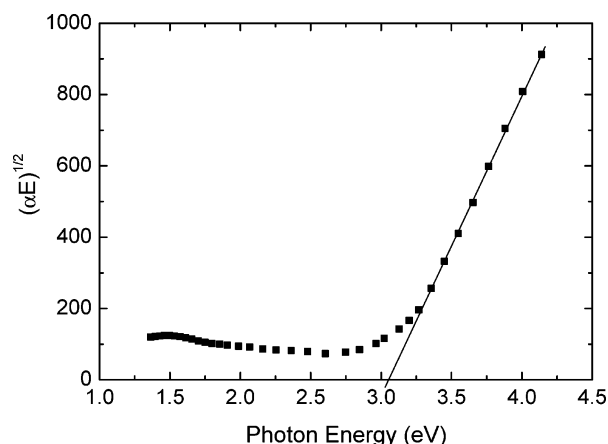


Figure 10. Plot of $(\alpha E)^{1/2}$ as a function of E for a film deposited with $I_F = 12.5$ A and $F_{O_2} = 12$ sccm.

E_g -values for all films of the series, calculated using the same procedure, are listed in Table 1. From Table 1, the optical gap does not exhibit any well-defined trend with the increase in the oxygen flow and averages to 3.03 eV. This result is in the interval of E_g -values of molybdenum oxide films deposited by reactive sputtering,^{6,10} CVD,^{13,40} and thermal evaporation.^{41,42} 2.7–3.2 eV.

Since the optical gap depends on the stoichiometry and structure of the Mo oxide investigated, a range of E_g -values have been reported in the literature for Mo oxide films, depending on the deposition method, deposition parameters, and film postdeposition treatment. In films obtained by reactive sputtering, for instance, the optical gap depends on the oxygen pressure in the deposition chamber and E_g -values in the range from 2.3 to 3.2 eV, increasing with the increase in the oxygen flow rate to the chamber, have been reported.^{10,43} From Table 1, however, there is no systematic change in E_g

(38) Jagadeesh M. S.; Damodura, D. V. *J. Non-Cryst. Solids* **1978**, 28, 327.

(39) Tauc, J. In *The Optical Properties of Solids*; Abeles, F., Ed.; North-Holland: Amsterdam, 1972.

(40) Abdellaoui, A.; Martin, L.; Donnadieu, A. *Phys. Status Solidi A* **1988**, 109, 455.

(41) Deb, S. K. *Proc. R. Soc. A* **1968**, 304, 211.

(42) Quevedo-Lopez, M. A.; Reidy, R. F.; Orozco-Teran, R. A.; Mendoza-Gonzales, O.; Ramirez-Bon, R. *J. Mater. Sci. Mater. Electron.* **2000**, 11, 151.

(43) Cruz, T. G. S.; Gorenstein, A.; Landers, R.; Kleiman, G. G.; de Castro, S. C. *J. Electron Spectrosc. Relat. Phenom.* **1999**, 101–103, 397.

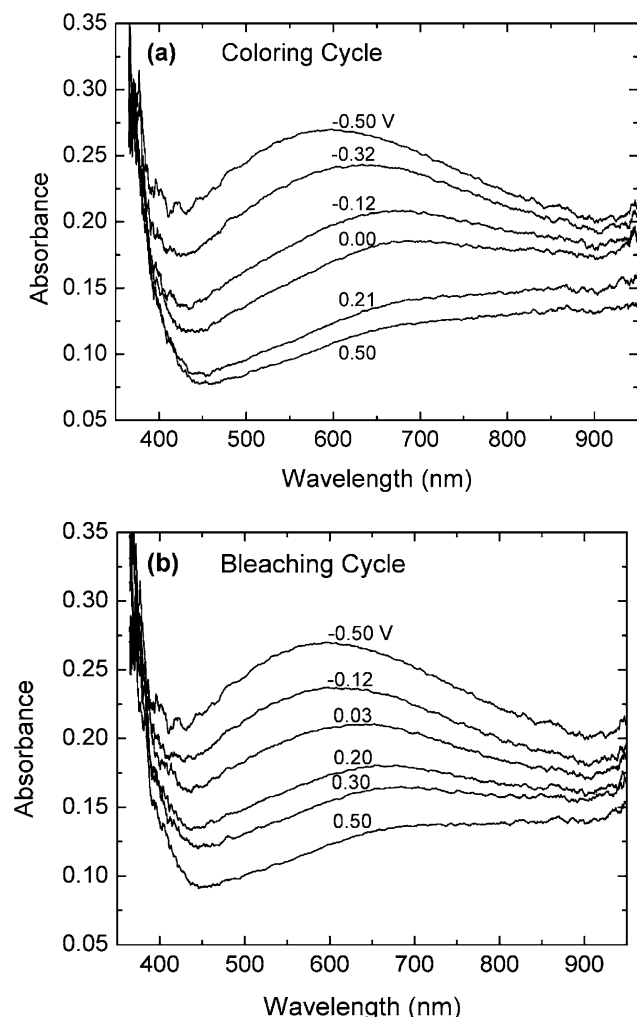


Figure 11. Absorbance spectra for various cell potentials for a film prepared with the filament current of 11 A and the oxygen flow rate of 18 sccm. Measurements were performed at constant current densities of $-6.25 \mu\text{A}/\text{cm}^2$ for Li^+ insertion (a) and $+6.25 \mu\text{A}/\text{cm}^2$ for Li^+ extraction (b).

with F_{O_2} . Consistent with the RBS and XPS results, this implies that within the F_{O_2} -range investigated, there is no significant difference in the composition and structure of the films.

Electrochromism. The electrochromic effect was observed by inserting and extracting electrons and Li^+ ions electrochemically in the molybdenum oxide films, using the chronopotentiometric technique⁴⁴ at a constant counter electrode current. Changes in the optical absorbance under Li^+ intercalation for a film prepared using a filament current of 11 A and an oxygen flow rate of 18 sccm are shown in Figure 11a,b. The former correspond to Li^+ insertion (coloring cycle) and the latter to Li^+ extraction (bleaching cycle). In each cycle, the current continuously circulated in the cell while the cell potential, V_c , varied between -0.50 and $+0.50$ V over 1040 s. The various spectra shown in the figures were taken at different V_c -values and the acquisition time of each spectrum was approximately 1 ms.

The spectrum for $V_c = +0.50$ V, shown in Figure 11a, corresponds to the nonintercalated film. After the intercalation process was initiated, the absorbance, for

any wavelength in the 400–900-nm range, increased as V_c decreased from $+0.50$ to -0.50 V, due to Li^+ ion insertion. For Figure 11b, the data were taken with the same current magnitude as in Figure 11a, but with opposite sign, starting at $V_c = -0.50$ V. As the Li^+ ions were extracted, the absorbance decreased and V_c increased from -0.50 to $+0.50$ V. Comparison of (a) and (b) of Figure 11 reveals that complete reversibility of the optical absorbance was not obtained in the bleaching cycle at the potential of $+0.5$ V because a residual charge remained trapped in the film, producing an optical absorbance higher than that observed in the nonintercalated state.

One of the relevant parameters used to characterize an electrochromic film is the coloration efficiency,⁴⁵ defined as $\eta = \Delta A / \Delta \rho$ where ΔA is the change in the optical absorbance at a given wavelength promoted by the insertion or extraction of a charge ΔQ corresponding to a charge density $\Delta \rho$, defined as the charge per unit area of the film. Using the data of Figure 11a for the wavelength of 700 nm, calculating ΔA as the difference between the absorbances at the cell potentials of $+0.50$ and -0.50 V, and evaluating $\Delta \rho$ as the current density multiplied by the time interval taken to produce the change ΔA , one obtains $\eta = 19.5 \text{ cm}^2/\text{C}$, a value similar to that obtained by other investigators ($22 \text{ cm}^2/\text{C}$) at the same wavelength for as-deposited Mo oxide films obtained by electrodeposition.⁴⁶ It is known, however, that the electrochromic properties of Mo oxide films may be improved by thermal treatment.^{14,46} In ref 46, for example, it is reported that the η -values were changed from 22 to $41 \text{ cm}^2/\text{C}$ upon annealing at 533 K. Investigations of thermally treated molybdenum oxide films obtained by HFMOD, aiming to improve the coloration efficiency, are underway.

Conclusions

Molybdenum oxide films were obtained using a novel technique, based on the formation of volatile oxide species from the surface of a heated molybdenum filament, from reactions between oxygen and molybdenum. The film deposition rate was studied as a function of the oxygen flow rate and the molybdenum filament current and temperature. Deposition rates as high as 31 nm min^{-1} were observed. Amorphous, compact, and uniform films, exhibiting good adhesion to glass and silicon substrates, were obtained by this technique.

Analysis by FTIR spectroscopy with a p-polarized radiation beam revealed some important structural details of the molybdenum oxide film structure which are not observed if the “regular” FTIR technique (with a nonpolarized beam) is used.

From the XPS data, it was concluded that the Mo atoms were in mixed valence states, Mo^{6+} and Mo^{5+} with a high predominance of the former over the latter. Thus, the film was in the overall MoO_x stoichiometry, with x smaller but close to 3. This result was supported by the RBS data, yielding an average atomic ratio of 2.9, consistent with an oxygen-deficient MoO_3 film. The ratio of the O atoms bound to Mo atoms was actually

(45) Zhang, J. G.; Benson, D. K.; Tracy, C. E.; Deb, S. K.; Czanderna, A. W. *J. Electrochem. Soc.* **1997**, *144*, 2022.

(46) Guerfi, A.; Paynter, R. W.; Dao, L. H. *J. Electrochem. Soc.* **1995**, *142*, 3457.

(44) Bard, A. J.; Faulkner, L. R. *Electrochemical Methods: Fundamentals and Applications*; John Wiley and Sons: New York, 1980.

smaller than 2.9 since, as revealed by the FTIR analysis, water was absorbed by the films and the O atoms from water contribute to the total oxygen RBS signal. Both the XPS and the RBS analyses performed on films obtained with the same filament current and over a wide range of oxygen flow rates did not reveal any trend in structural details and composition as the oxygen flow rate varied. The observation that the film stoichiometry is close to that of MoO_3 is consistent with the expectation that the film is formed from MoO_3 and MoO_2 species desorbed from the Mo filament and that the desorption rate of the former is greater than that of the latter.

An average value of 3.03 eV was found for the optical gap of a number of films prepared with the same filament current and various oxygen flow rates. Similarly to the XPS and RBS results, no trend in the E_g values was found as the oxygen flow rate was varied.

All films investigated in the electrochemical cell exhibited the electrochromic effect upon Li^+ intercalation. From detailed absorbance measurements on one

of the samples, a coloration efficiency of $19.5 \text{ cm}^2/\text{C}$ at 700 nm was measured.

Acknowledgment. The authors thank the Fundação de Amparo à Pesquisa do Estado de S. Paulo-FAPESP (Grants 02/07482-6 and 98/10979-2) and the Conselho Nacional de Desenvolvimento Científico e Tecnológico (CNPq) for financial support. Thanks are also due to Drs. L. Cescatto and C. U. Davanzo for allowing the utilization of equipment under their supervision (electron scanning microscope and FTIR spectrometer, respectively) and to Drs. L. P. Cardoso and M. C. Fantini, the latter from the University of S. Paulo, for clarifying discussions concerning X-ray analysis. E. L. Rigon, R. C. G. Vinhas, and J. A. Fraymann provided excellent technical assistance with the SEM, XPS, and XRD analyses, respectively.

CM034551A